Effect of Cross-Linking on the Structure and Thermodynamics of Lamellar Block Copolymers

Enrique D. Gomez,[†] Jayajit Das,[†,‡] Arup K. Chakraborty,*[,†,‡,§,⊥] John A. Pople,[||] and Nitash P. Balsara*[,†,‡,#]

Department of Chemical Engineering, University of California, Berkeley, California 94720, Materials Sciences Division, Lawrence Berkeley National Laboratory, Berkeley, California 94720, Department of Chemistry, University of California, Berkeley, California 94720, Physical Biosciences Division, Lawrence Berkeley National Laboratory, Berkeley, California 94720, Stanford Synchrotron Radiation Laboratory, SLAC, P O Box 4349, Stanford, California 94309, and Environmental Energy and Technologies Division, Lawrence Berkeley National Laboratory, Berkeley, California 94720

Received October 29, 2005; Revised Manuscript Received March 10, 2006

ABSTRACT: Small-angle X-ray scattering, depolarized light scattering, and transmission electron microscopy were used to study the dependence of structure and thermodynamics on cross-linking of a symmetric poly(styrene-*block*-isoprene) copolymer. The polyisoprene block was cross-linked well above the order−disorder transition (ODT) temperature of the un-cross-linked block copolymer. A mean-field theory based on a coarse grained free energy and an RPA-like formulation was developed to predict the dependence of the ODT temperature on cross-linking density. Our theory is limited to cross-linking densities below the gel point. In both experiments and theory the ODT temperature increases as the number of junctions is increased for cross-linking densities below the gelation point. We show that reversible order−disorder transitions are obtained in these materials even when the cross-linking density is larger than that required to obtain a gel. At cross-linking densities near the gel point, the depolarized light scattering signal from the ordered state suddenly increases by orders of magnitude due to the presence of extremely long and thin grains. At sufficiently high cross-linking densities, the disordered state is trapped, and order−disorder transitions are no longer obtained.

Introduction

Cross-linking is a standard reaction used to solidify polymer liquids.[1,2] Recent studies have shown that cross-linking can be used to fix molecular aggregates such as individual micelles[3−7] and ordered arrays of block copolymer mesophases.[8−10] In earlier work, we conducted experiments to study the possibility of obtaining reversible order−disorder transitions in cross-linked diblock copolymer melts.[11,12] In refs 11 and 12, the polyisoprene block of a poly(styrene-*block*-isoprene) copolymer with cylindrical morphology (polystyrene cylinders in a polyisoprene matrix) was cross-linked in the disordered state. We observed order−disorder transitions in these materials at cross-linking densities in excess of that required to obtain a gel. We thus obtained a reversible transition from an ordered solid to a disordered solid, in contrast to conventional block copolymers that exhibit a transition from an ordered solid to a disordered liquid.

There has been considerable theoretical progress in our understanding of the phase behavior of cross-linked homopolymers[2,13−15] and the microphase separation in un-cross-linked block copolymer systems.[16,17] However, combining these theoretical constructs to address the phase behavior of cross-linked block copolymers remains a challenging problem. In particular, there are no predictions for the dependence of the order−disorder transition temperature of block copolymers on cross-linking density. Phenomenological Landau−Ginzburg free energy functionals have been proposed to study the domain morphology in ordered phases in cross-linked block copolymers.[18,19] Monte Carlo simulations have also been employed to investigate the effect of cross-links introduced in the ordered phase in block copolymer melts.[20] In this paper, we derive an expression for the coarse grained free energy density of cross-linked block copolymers based on formulations by Leibler,[16] Deam and Edwards.[13] Unfortunately, this approach cannot be extended to study the gel phases due to the presence of nonintensive terms in the free energy density beyond the gelation point.

Small-angle X-ray scattering, depolarized light scattering, and transmission electron microscopy experiments were conducted on a cross-linked, symmetric poly(styrene-*block*-isoprene) copolymer. At cross-linking densities below the gel point, we compare experimentally determined ODTs with theoretical predictions. Our experiments at higher cross-linking densities establish that reversible order−disorder transitions can be obtained in cross-linked block copolymer solids with lamellar order. However, there are some striking differences between the cross-linked lamellar samples studied here and the cylindrical samples studied in refs 11 and 12. In particular, there is evidence of an unusual grain structure near the gelation point. We conclude with a discussion of the temperature vs cross-linking density phase diagram.

Theory

Consider a polymer melt of volume V with m A−B diblock copolymer chains, each of which consists of N monomers. The volume fraction of the un-cross-linked block, which we take to be the A block, is f. The Hamiltonian of the system is given by Edwards:[21]

[†] Department of Chemical Engineering, University of California, Berkeley.
[‡] Materials Sciences Division, Lawrence Berkeley National Laboratory.
[§] Department of Chemistry, University of California, Berkeley.
[⊥] Physical Biosciences Division, Lawrence Berkeley National Laboratory.
[||] Stanford Synchrotron Radiation Laboratory.
[#] Environmental Energy and Technologies Division, Lawrence Berkeley National Laboratory.

10.1021/ma052323r CCC: $33.50
Published on Web 06/10/2006

$$H/k_BT = \sum_{i=1}^{m} \frac{3}{2Nl_0^2} \int_0^1 ds \left(\frac{dr_i}{ds}\right)^2 + V(\{r_i\}) \quad (1)$$

where $r_i(s)$ describes the configurations of the ith chain in three dimensions and l_0 is the Kuhn length. The excluded volume interactions between the monomers are described by[16]

$$V(\{r_i\}) = \sum_{i,j=1}^{m} \sum_{a,b=(A,B)} \frac{v_{ab}N^2}{2} \int_a ds \int_b ds' \delta(r_i(s) - r_j(s')) \quad (2)$$

where $\int_A \equiv \int_0^f$ and $\int_B \equiv \int_f^1$. The strengths of the couplings between $A-A$, $B-B$ and $A-B$ monomers are v_{AA}, v_{BB} and $v_{AB(BA)}$, respectively. The excluded volume interactions are conveniently described in terms of the Flory−Huggins parameter,[16,22] $\chi = (v_{AB} - (v_{AA} + v_{BB})/2)v_0^{-1}$, which is observed to vary as $A + B/T$ in experiments,[23] where A and B are system dependent parameters. Since we cross-link only one of the blocks experimentally, let us consider that there are R cross-links between the B blocks of AB diblock copolymers. Each cross-link constrains the movements of the monomers involved in the cross-link. If the s_l segment of the chain, i_l, is cross-linked with the s'_l segment of the i'_lth chain, then constraints due to the cross-links can be represented by $\delta(r_{i_l}(s_{i_l}) - r_{i'_l}(s'_l))$. Since the cross-links are permanent, the partition function of the system will depend on the cross-link distribution of the system. Thus, the partition function will be given by[13]

$$Z(\{i_l, s_l; i'_l, s'_l\}) = \mathcal{N} \int D(\{r_i\}) \prod_{l=1}^{R} \int_{Nf}^{N} ds_l \int_{Nf}^{N} ds'_l \delta(r_{i_l}(s_l) - r_{i'_l}(s'_l)) \exp(-\beta H) \quad (3)$$

where the normalization is given by $\mathcal{N}$.[24] However, as in other systems with quenched disorder, it is not straightforward to extract the thermodynamically interesting quantities from the above form of the partition function. Therefore, one can use the self-averaging property of the system to average $\ln(Z)$ over a probability distribution of the quenched disorder (for example, cross-links in our system) to calculate a free energy of the system.[25,26] This is effectively done by the standard replica method which utilizes the identity $\ln(Z) = Lt_{n\to 0}(Z^n - 1)/n$.[27] The probability distribution for a particular set of cross-links can be described by $P_R(\{i_l,s_l;i'_l,s'_l\}) \propto \prod_{l=1}^{R} v_0\delta(r_{i_l}(s_l) - r_{i'_l}(s'_l))$, where v_0 is a reference volume. Instead of taking a fixed number of cross-links in the system, it will be convenient in dealing with calculations without any loss of generality to assume that the cross-links follow a Poisson distribution with the number of cross-links being equal to R.[28] After the inclusion of the fluctuations in the total number of cross-links and considering the fact that the conformations of the cross-linked chains correspond to equilibrium configurations of the system,[29] the probability distribution of the cross-links can be described by

$$P_R(\{r_{i_l}(s_l); r_{i'_l}(s'_l)\}) = \frac{\mathcal{A}}{R!}\left(\frac{\mu^2}{2}\right)^R \int D(\{r_i\}) \exp(-\beta H) \prod_{l=1}^{R} v_0 \delta(r_{i_l}(s_l) - r_{i'_l}(s'_l)) \quad (4)$$

In the above equation, $\mathcal{A}$ is the normalization constant and the parameter μ determines the average number of cross-links in the Poisson distribution in the following manner: $\mu^2(1-f)^2N/2 \approx \langle R\rangle/m$, which is also the average number of cross-link per chain (details are presented in Appendix A), and $\langle ...\rangle$ denotes an average over the distribution in eq 4. The free energy of the system can be calculated from

$$F = -\beta^{-1}\overline{\ln(Z)} = -\beta^{-1} \underset{n\to 0}{Lt} \frac{Z_{n+1} - Z_1}{nZ_1} = \underset{n\to 0}{Lt} \frac{F_n}{n} \quad (5)$$

where Z_{n+1}, the partition function for $n+1$ replica systems, is defined as

$$\begin{aligned} Z_{n+1} &= \mathcal{N} \int \left(\prod_{\alpha=0}^{n} D(\{r_i^\alpha\})\right) \prod_{\alpha=0}^{n} \sum_{R=1}^{\infty} \frac{1}{R!}\left(\frac{\mu^2}{2}\right)^R \times \\ &\sum_{i_l=1}^{m} \sum_{i'_l=1}^{m} \left(\prod_{l=1}^{R} \int_{Nf}^{N} ds_l \int_{Nf}^{N} ds'_l v_0 \delta(r_{i_l}^\alpha(s_l) - r_{i'_l}^\alpha(s'_l))\right) \exp(-\beta H^{(\alpha)}) \\ &= \mathcal{N} \int \left(\prod_{\alpha=0}^{n} D(\{r_i^\alpha\})\right) \exp\left(-\sum_{\alpha=0}^{n} \beta H^{(\alpha)} + \frac{\mu^2 N^2}{2} \times \right. \\ &\left. \sum_{i,j}^{m} \int_f^1 ds \int_f^1 ds' \prod_{\alpha=0}^{n} v_0 \delta(r_i^\alpha(s) - r_j^\alpha(s'))\right) \quad (6) \end{aligned}$$

In the above equation, $r_i^\alpha(s)$ denotes the chain configurations in the αth replica system, where $H^{(\alpha)}$ denotes the Edwards Hamiltonian of that system. The cross-links couple the replica systems, giving rise to the second term in the parentheses in the above equation. Also note there are $n+1$ replica systems, because the 0th replica system acts as the reference ensemble where the cross-links were introduced and the distribution of cross-links is chosen from that reference ensemble. To develop a coarse grained description of the system we introduce microscopic density functions

$$\tilde{\rho}_A(\hat{r}) = N\sum_{i=1}^{m} \int_0^f ds \prod_{\alpha=0}^{n} v_0 \delta(r^\alpha - r_i^\alpha(s)) = N\sum_{i=1}^{m} \int_0^f ds\, v_0^{n+1} \delta(\hat{r} - \hat{r}_i(s))$$

and

$$\tilde{\rho}_B(\hat{r}) = N\sum_{i=1}^{m} \int_f^1 ds \prod_{\alpha=0}^{n} v_0 \delta(r^\alpha - r_i^\alpha(s)) = N\sum_{i=1}^{m} \int_f^1 ds\, v_0^{n+1} \delta(\hat{r} - \hat{r}_i(s))$$

The densities in the αth replica system are $\tilde{\rho}_{(A,B)}^\alpha(r^\alpha) = v_0^{-n} \int d\hat{x} \tilde{\rho}_{(A,B)}(\hat{x}) \delta(x^\alpha - r^\alpha)$. The density variables, $\rho_{(A,B)}^\alpha(r^\alpha)$, describing a replica system are a subset of the density variables $\rho_{(A,B)}(\hat{r})$. The melt can be considered incompressible,[16] i.e., $\tilde{\rho}_A^\alpha + \tilde{\rho}_B^\alpha = 1$, which implies that the reference volume, v_0, is the volume of a single monomer. In the above equations, a $3(n+1)$ dimensional vector space spanned by $\hat{r} = \{r^0, r^1, ..., r^n\}$ is introduced to keep the notation simple and compact. The interaction term describing the coupling between the replica systems, when described in terms of the density variables, $\tilde{\rho}_{(A,B)}(\hat{r})$, assumes the standard form of an excluded volume interaction, $\mu^2/2v_0^{n+1} \int d\hat{r} \tilde{\rho}_B(\hat{r}) \tilde{\rho}_B(\hat{r})$. We introduce identities, $1 = \int D\rho_{(A,B)} \delta(\rho_{(A,B)} - \tilde{\rho}_{(A,B)})$, in the partition function in order to derive a free energy in terms of the coarse grained density functions, $\rho_{(A,B)}(\hat{r})$. Since we are interested in studying the ordering transition in the system, the free energy is calculated

in terms of the order parameter, $\psi(\hat{r}) = (1 - f)\rho_A(\hat{r}) - f\rho_B(\hat{r})$, and the total density, $c(\hat{r}) = \rho_A(\hat{r}) + \rho_B(\hat{r})$. In the disordered phase, $\psi^\alpha(r^\alpha) = 0$, and in the ordered phases, $\psi^\alpha(r^\alpha)$ assumes nonzero values. The cross-links can give rise to "amorphous solid" phases,[28] where an analogue of the Edwards−Anderson order parameter for spin glasses can be used to characterize the phase. For example, $c(0,k,-k,0,...,0)$,[28] where $c(k^0,k^1,k^2,...,k^n)$ is the Fourier transform of $c(\hat{r})$, can be used to characterize the "amorphous solid state". In general, the density variable $c(\hat{k})$, Fourier transform of $c(\hat{r})$, can be split in the following manner

$$c(\hat{k}) = c(\hat{k})\delta_{\hat{k},0} + c(\hat{k})(1 - \delta_{\hat{k},0}) \times (\sum_{\alpha=0}^{n}\prod_{\beta=0,\beta\neq\alpha}^{n}\delta_{k^\beta,0}) + c(\hat{k})(1 - \delta_{\hat{k},0})(1 - \sum_{\alpha=0}^{n}\prod_{\beta=0,\beta\neq\alpha}^{n}\delta_{k^\beta,0}) = c_0(\hat{k}) + c_1(\hat{k}) + \bar{c}(\hat{k}) \quad (7)$$

The first term $c_0(\hat{k})$ in the above equation is nonzero when all elements in $\{k^\alpha\}$ are zero and we can say $c_0(\hat{k})$ belongs to the zero replica sector. The second term, $c_1(\hat{k})$, would fall in the first replica sector, where all but one of $\{k^\alpha\}$ is zero. $c_1(\hat{k})$ would denote the densities $\{c^\alpha(k^\alpha)\}$ in replica systems. The last term $\bar{c}(\hat{k})$ resides in the higher replica sector, where more than one of $\{k^\alpha\}$ are nonzero. The presence of a nonzero higher replica sector in $c(\hat{k})$ would reflect coupling between different replica systems. The liquid phase or the amorphous solid phase is identified in the nonvanishing components of the one or higher replica sector of the density variable $c(\hat{k})$.

We follow the standard Random Phase Approximation (RPA) scheme to derive the free energy as a polynomial in the density fields, $\psi(\hat{r})$ and $c(\hat{r})$.[16,30] The details of the calculations are provided in Appendix B. The free energy, F_n, to quadratic order in $\psi(\hat{k})$ and $c(\hat{k})$, Fourier transforms of $\psi(\hat{r})$ and $c(\hat{r})$, respectively, is given by

$$F_n = \int\frac{d\hat{k}}{(2\pi)^{3(n+1)}}(\Gamma_{\psi\psi}\psi(\hat{k})\psi(-\hat{k}) + \Gamma_{\psi c}\psi(\hat{k})c(-\hat{k}) + \Gamma_{cc}c(\hat{k})c(-\hat{k})) + O(\psi^3,c^3,c\psi^2,\psi c^2) \quad (8)$$

where

$$\Gamma_{\psi\psi} = \frac{V^{n+1}}{m(N{v_0}^{n+1})^2D}(f^2g_2(fx) + (1 - f)^2g_2((1 - f)x) + 2f(1 - f)g_{12}(fx,(1 - f)x)) - \frac{\mu^2}{2{v_0}^{n+1}} - \frac{1}{{v_0}^{2n+1}}\sum_{\alpha=0}^{n}\chi^{(\alpha)}\prod_{\beta=0,\beta\neq\alpha}^{n}\delta(k^\beta) \quad (9)$$

$$\Gamma_{c\psi} = \frac{V^{n+1}}{m(N{v_0}^{n+1})^2D}(fg_2(fx) + (1 - f)g_2((1 - f)x) + (1 - 2f)g_{12}(fx,(1 - f)x)) - \frac{(1 - f)\mu^2}{2{v_0}^{n+1}} + \frac{1}{{v_0}^{2n+1}}\sum_{\alpha=0}^{n}u^{(\alpha)}\prod_{\beta=0,\beta\neq\alpha}^{n}\delta(k^\beta) \quad (10)$$

and

$$\Gamma_{cc} = \frac{V^{n+1}}{2m(N{v_0}^{n+1})^2D}(f^2g_2(fx) + (1 - f)^2g_2((1 - f)x) - 2f(1 - f)g_{12}(fx,(1 - f)x)) - \frac{(1 - f)^2\mu^2}{2{v_0}^{n+1}} + \frac{1}{{v_0}^{2n+1}}\sum_{\alpha=0}^{n}w^{(\alpha)}\prod_{\beta=0,\beta\neq\alpha}^{n}\delta(k^\beta) \quad (11)$$

Here $D = f^2(1 - f)^2[g_2(fx)g_2((1 - f)x) - (g_{12}(fx,(1 - f)x))^2]$ and $x = Nl_0^2(\hat{k}.\hat{k})/6$. $g_2(y) = 2/y^2(y + \{\exp(-y) - 1\})$ is the Debye function and $g_{12}(x,y) = 1/(xy)(1 + \exp(-x - y) - \exp(-x) - \exp(-y))$. The parameters $u^{(\alpha)}$ and $w^{(\alpha)}$ are given by $u^{(\alpha)} = (fv_{AA}^{(\alpha)} - (1-2f)v_{AB}^{(\alpha)} + (1 - f)v_{BB}^{(\alpha)})/v_0$ and $w^{(\alpha)} = (f^2v_{AA}^{(\alpha)} + 2f(1 - f)v_{AB}^{(\alpha)} + (1 - f)^2v_{BB}^{(\alpha)})/2v_0$, where $v_{AA}^{(\alpha)}$, $v_{BB}^{(\alpha)}$ and $v_{AB}^{(\alpha)}$ are the strengths of interactions between the A and B type monomers in the αth replica system. The function $\Gamma_{cc} \rightarrow V^{n+1}/(2m(N{v_0}^{n+1}))^2 - (1 - f)^2\mu^2/(2{v_0}^{n+1}) + O(\hat{k}.\hat{k})$ as $\hat{k}\cdot\hat{k} \rightarrow 0$. Therefore, in the limit $n \rightarrow 0$, $\Gamma_{cc} < 0$ as $(1 - f)^2\mu^2N > 1$. This implies that if the average number of cross-links per chain is higher than 0.5, the liquid state described by $\bar{c}(\hat{k}) = 0$ becomes unstable, and a state with $\bar{c}(\hat{k}) \neq 0$ is likely to describe a new phase. However, extension of this formalism for regimes where the average number of cross-links is higher than 0.5 gives rise to unphysical, nonintensive terms proportional to $\ln(V)$ in the free-energy density.[28] Therefore, we restrict our study to the liquid phase where the formalism works well. The change in T_{ODT} can be calculated from $\Gamma_{\psi\psi}(\hat{k})$ (details provided in Appendix B), which can be approximated, as in a melt of diblock copolymers, as $\Gamma_{\psi\psi}(\hat{k}) = (n + 1)V^{n+1}\chi_{min}/(2m(N{v_0}^{n+1})^2) - \mu^2/(2{v_0}^{n+1}) - 1/{v_0}^{2n+1}\sum_{\alpha=0}^{n}\chi^{(\alpha)}\prod_{\beta=0,\beta\neq\alpha}^{n}\delta(k^\beta) + O((k - k_m)^2)$. Here $k_m^\alpha \propto 1/(Nl_0^2)^{1/2}$ is the wave vector which determines the phase separation length scale and χ_{min} is the minimum value of the k^α dependent part of $\Gamma^{(\alpha)}(k^\alpha)$. The $\alpha = 0$ replica system refers to the reference system where the cross-links were introduced. The temperatures, determined by $\chi^{(\alpha)}$, at the $\alpha = 0$ replica systems refer to the temperature of the cross-linked system. Below the ordering transition, $\Gamma_{\psi\psi}(\hat{k}_m) < 0$, we obtain nonzero $\psi^\alpha(k^\alpha)$ as the stable solutions of the system. The free energy, F, is calculated by letting $n \rightarrow 0$ as shown in eq 5. The value of the product χN at the microphase ordering transition for the cross-linked system, $(\chi N)_{ODT}^{cr}$, is found by obtaining solutions for $F_n = F_n(\bar{c}(\hat{k}) = 0,\psi(\hat{k}) = 0)$ (eqs 8−11, we derive these equations in Appendix B), where $F_n(\bar{c}(\hat{k}) = 0,\psi(\hat{k}) = 0)$ denotes the value of the free energy F_n in the disordered liquid state for nonzero values of the order parameter. We obtain

$$(\chi N)_{ODT}^{cr} = (\chi N)_{ODT} - \frac{n_{c,gel}X_c}{(1 - f)^2} \quad (12)$$

where $X_c = n_c/n_{c,gel}$ and $n_c = (1 - f)^2\mu^2N/2$ is the average number of cross-links per chain. The number of cross-links required to form a gel, $n_{c,gel}$, is taken to be 0.5.[1,28] The microphase ordering transition temperature of the cross-linked system (T_{ODT}^{cr}) is given by

$$T_{ODT}^{cr} = \frac{T_{ODT}}{1 - \frac{X_cT_{ODT}}{2N(1 - f)^2B}} \quad (13)$$

where T_{ODT} is the ordering temperature of the un-cross-linked system, and we have assumed that the Flory−Huggins parameter

is given by $\chi = A + B/T$. Derivations of the above equations (eq 12 and eq 13) are shown in Appendix B.

Equations 12 and 13, which describe the effect of cross-linking on the stability of the disordered phase, are the main result of our theoretical analysis. Intuitively one might anticipate that cross-linking in the disordered phase would tend to stabilize the disordered phase. Equations 12 and 13 indicate that the opposite is true, i.e., cross-linking in the disordered phase leads to the stabilization of the ordered phase. This is because selectively cross-linking the B blocks results in correlations between the B monomers that are absent in the un-cross-linked sample. This promotes order formation. In addition, eq 12 shows that the rate of change of $(\chi N)_{ODT}^{cr}$ with respect to the cross-linking density is inversely proportional to the square of the volume fraction of the cross-linked component. Therefore, the order−disorder transition temperature of systems in which the volume fraction of the un-cross-linked block, *f*, is higher will be more sensitive to changes in the cross-linking density. Also, it is evident from eq 13 that the dependence of the order−disorder transition temperature on cross-linking density is more dramatic when the B parameter is small. Of course, the tendency for promoting order formation is only applicable below the gel point. Several theories show that monomers in cross-linked samples are localized within a region of size ξ, which decreases as the cross-link density increases.[28,31,32] Microphase ordering, which occurs at a length scale proportional to the chain radius of gyration, R_g, can only occur within regions of size ξ. We would expect that as ξ decreases to length scales smaller than R_g, the localization of monomers will hinder microphase separation, and the disordered phase will be trapped by cross-linking. Our efforts to extend the theory into this regime were unsuccessful due to difficulties described above.

Experimental Details

A poly(styrene-*block*-isoprene) copolymer was synthesized using methods described previously.[23] The resulting polymer was characterized using gel permeation chromatography (GPC) of the precursor block and GPC and ^{1}H NMR of the final polymer. The weight-averaged molecular weights of the polystyrene and polyisoprene blocks were determined to be 10 and 9 kg mol^{-1}, respectively; the polydispersity index of the polymer = 1.02. We refer to this polymer as SI(10−9). The volume fraction of the polystyrene block, *f*, was 0.50. The glass transition temperature was found to be between 55 and 75 °C by differential scanning calorimetry (DSC).

Mixtures of about 1 g of SI(10−9) and dicumyl peroxide (DCP) were prepared by dissolving predetermined amounts of the components in benzene. The mixture was then freeze-dried for 24 h. The final DCP concentrations were determined by weighing the dry mixtures, and these concentrations were found to match the initial concentrations for all mixtures within our experimental error (±0.3 mg). The compositions of the samples are given in Table 1.

SI(10−9)/DCP mixtures were molded into disks with 7.5 mm diameter and 1 mm thickness using a Carver press at room temperature. The disks were placed in anodized aluminum spacers and annealed at 105 °C for 30 min prior to curing the sample at 160 °C for 2 h, under a N_2 blanket between 200 and 300 psi to prevent the formation of bubbles. This results in the selective cross-linking of the isoprene block.[12,33] Although the cross-linking reactions between DCP and polyisoprene are not simple, it is observed that at low concentrations one molecule of DCP creates one cross-linked site.[33]

The cross-linked samples were immersed in toluene and the amount of solvent uptake was determined for the samples which formed a gel. The polymer volume fractions at swelling equilibrium are tabulated in Table 1. After the swelling experiments, the gels were dried for 72 h under vacuum and the dry gels were weighed. The gel fraction, f_{gel}, defined as the ratio of the weight of the dry network before swelling to the weight after, is given in Table 1. Lacking a theory that addresses the swelling of cross-linked block copolymers,[12] the molecular weight between cross-links, M_c, was determined using expressions developed for imperfect homopolymer networks[34,35] and the affine network model for swelling equilibrium[35−37]

Table 1. Characteristics of Cross-Linked Samples

sample	DCP (wt %)	V_2[a]	gel fraction, f_{gel}	M_c[b]	$N_{c,affine}$[c]	$N_{c,DCP}$[d]	X_c[e]
SI[0.00]	0.00					0.00	0.00
SI[0.16]	0.32					0.22	0.16
SI[0.32]	0.63					0.43	0.32
SI[0.47]	0.93					0.64	0.47
SI[0.59]	1.17					0.81	0.59
SI[0.63]	1.25					0.87	0.63
SI[0.76]	1.51					1.05	0.76
SI[0.83]	1.64					1.14	0.83
SI[0.94]	1.85					1.29	0.94
SI[0.95]	1.88					1.31	0.95
SI[1.00]	1.97	0.0499	0.55	8.26	1.12	1.38	1.00
SI[1.02]	2.00	0.0540	0.57	8.15	1.13	1.40	1.02
SI[1.04]	2.05	0.0550	0.73	8.12	1.14	1.43	1.04
SI[1.07]	2.10	0.0557	0.84	8.09	1.14	1.47	1.07
SI[1.10]	2.16	0.0571	0.91	8.04	1.15	1.51	1.10
SI[1.15]	2.25	0.0641	0.80	7.86	1.18	1.57	1.15
SI[1.27]	2.48	0.0756	0.92	7.51	1.23	1.74	1.27
SI[2.20]	4.23	0.1563	0.88	4.90	1.88	3.02	2.20

[a] Polymer volume fraction in gel [b] Molecular weight between cross-links (kg/mol) based on the affine network model [c] Number of cross-links per chains based on the affine network model [d] Number of cross-links per chain based on the DCP concentration [e] Number of cross-links per chain based on the DCP concentration normalized over the experimentally determined gelation point

$$M_c = \frac{V_S\rho\left(\frac{\phi_p}{2} - \phi_p^{1/3}\right)}{\ln(1-\phi_p) + \phi_p + \chi_{SP}\phi_p^{\,2} + \frac{V_S\rho}{2M_n}(\phi_p - 4\phi_p^{1/3})} \quad (14)$$

where V_S is the solvent molar volume, ρ is the network density, χ_{SP} is the solvent−polymer interaction parameter, M_n is the number-average molecular weight, and ϕ_p is the polymer volume fraction at swelling equilibrium. Calculated M_c values are tabulated in Table 1.[38] We then calculate the number of cross-links per chain determined via swelling, $N_{c,affine}$, by

$$N_{c,affine} = \frac{2M_n}{\varphi M_c} \quad (15)$$

Here φ is the network functionality, and we assume it to be 4.[1,36] We also calculate the number of cross-links per chain based on the DCP wt %, $N_{c,DCP}$ (assuming each DCP molecule creates one cross-link[33]), and compare these cross-linking densities to those calculated by the swelling experiments in Table 1. For convenience, we express the cross-linking density in terms of X_c, which is $N_{c,DCP}$ normalized by $N_{c,DCP}$ at the gel point, and X_c values are given in the final column of Table 1. Samples are identified by the value of X_c; thus, SI[1.00] is the sample with the lowest DCP amount of the cross-linked block copolymers that form gels.

Depolarized light scattering (DPLS) experiments were conducted on 1 mm thick dry samples in an apparatus described in ref 39. All of the samples were equilibrated for 30 min at each temperature during both heating/cooling runs. The temperature steps were either 2 or 5 °C and the temperature range that we focus on is between 80 and 120 °C. We present values of the total forward DPLS power, *P*, normalized by the incident power, P_0, obtained as a function of temperature.[39] The temperature scans were repeated at least three times.

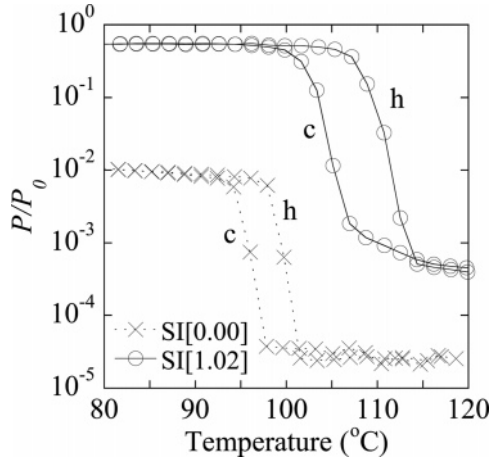

Figure 1. DPLS power vs temperature for SI[0.00] (crosses, dotted line) and SI[1.02] (open circles, solid line). The "c" next to the data denotes the cooling run, while the "h" denotes the heating run.

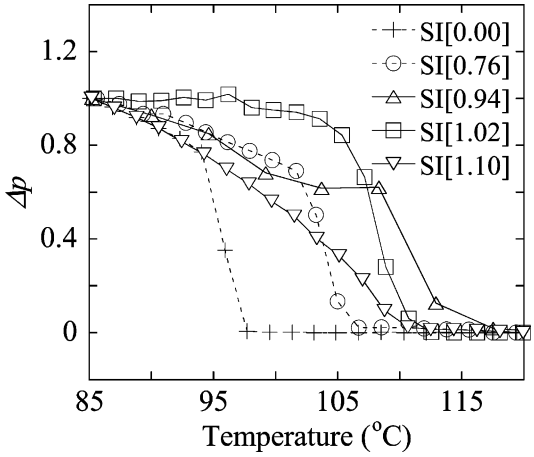

Figure 2. Normalized DPLS power vs temperature for various cross-linking densities, X_c, during heating runs. The DPLS power is normalized using eq 16.

SAXS experiments were performed at beamline 1−4 of the Stanford Synchrotron Radiation Laboratory with 1.488 Å wavelength photons as described in ref 40. Data were collected using a CCD-based X-ray detector, and the two-dimensional patterns were radially averaged over a 70° window. The data were corrected for the CCD dark current, and the scattering from air and Kapton windows. Absolute scattering intensities from a disordered SI(8−26) (an internal calibration sample) were determined using small-angle neutron scattering at the National Institute of Standards and Technology at temperatures between 132 and 168 °C. During the first SAXS experimental run, a T-independent calibration constant of the SAXS instrument was determined by comparing the SAXS and SANS measurements from SI(8−26) over the above temperature range. The SAXS intensity of a secondary polyethylene standard at room temperature was also measured during that run. The polyethylene standard was used to calibrate the SAXS instrument in subsequent experiments. Independent checks on well-studied disordered block copolymers indicated that our procedure for absolute calibration was accurate to within 10%.[41] The conclusions in this paper are based entirely on peak width analysis and thus not dependent on the uncertainties associated with the use of secondary standards for instrument calibration.[42]

Ultrathin sections (ca. 50 nm) were prepared for transmission electron microscopy (TEM) experiments using an RMC Boeckeler PT XL Ultramicrotome at −100 °C using a cryogenic attachment. The contrast between the polystyrene and polyisoprene domains was enhanced using 2 wt % (aq) OsO_4 vapor staining. Imaging was done at the National Center for Electron Microscopy (NCEM), Lawrence Berkeley National Laboratory using a JEOL 200CX microscope operating at 100−200 kV.

Results and Discussion

The depolarized light scattering signal, P/P_0, vs temperature for neat SI(10−9) ($X_c = 0.00$) and the sample with $X_c = 1.02$ is presented in Figure 1. The heating and cooling run data from the SI[0.00] are unremarkable with P/P_0 values of about 10^{-2} at low temperatures. The discontinuous decrease in P/P_0 at 98 ± 3 °C during the heating run is a standard signature of the order-to-disorder transition.[43] The formation of order seen during the cooling run requires undercooling the sample about 3 °C below T_{ODT}, the order−disorder transition temperature, and is typical of systems undergoing reversible first order phase transitions. Qualitatively similar data were obtained from the cross-linked samples. Typical data obtained from the SI[1.02] sample is shown in Figure 1. Here again we see a discontinuous drop in P/P_0 during the heating run at 111 ± 4 °C. We take this as a measure of the order−disorder transition temperature of our cross-linked sample, T_{ODT}^{cr}. The order, which is lost upon heating, reappears upon cooling, as shown in Figure 1. The order−disorder transition obtained in cross-linked samples above the gel point ($X_c > 1.00$) is thus reversible. As depicted in Figure 1, the ODT becomes less sharply defined as a result of the introduction of cross-links. For $X_c = 0$, the birefringence signal decreases over a temperature window of 4 °C, but for $X_c = 1.02$, this decrease occurs over a 7 °C temperature window. Another noteworthy observation is the difference in P/P_0 values obtained from the cross-linked and un-cross-linked samples. In the ordered state, P/P_0 for the SI[1.02] sample is about a factor of 100 larger than that obtained from the un-cross-linked sample. Possible reasons for this large difference will be addressed shortly.

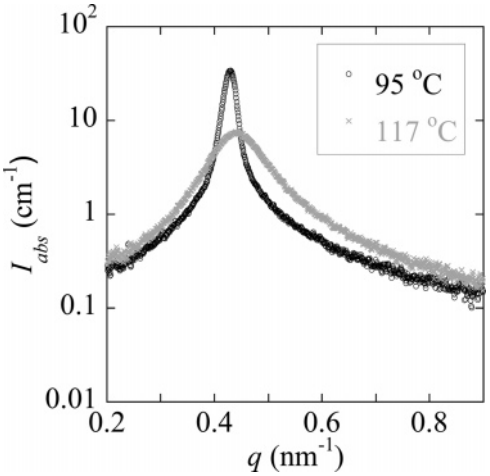

Figure 3. SAXS intensity, I, vs scattering vector, q, profiles for SI[1.02] at 95 °C (below the T_{ODT}) and 117 °C (above the T_{ODT}).

Figure 2 shows the DPLS power vs temperature for various cross-linking densities. To show all of the data on one plot, we present the normalized DPLS signal, Δp, defined as

$$\Delta p = \frac{P/P_0 - (P/P_0)_{120°C}}{(P/P_0)_{85°C} - (P/P_0)_{120°C}} \tag{16}$$

Although both heating and cooling scans were performed, only heating curves are shown for clarity. It is obvious from Figure 2 that T_{ODT}^{cr} increases with X_c at low values of X_c.

Figure 3 shows SAXS profiles for the SI[1.02] sample. The absolute scattering intensity, I, is plotted vs scattering vector q ($q = 4\pi \sin(\theta/2)/\lambda$, λ is the X-ray wavelength and θ is the

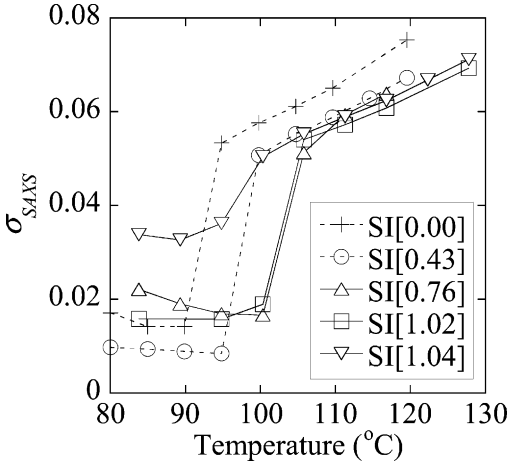

Figure 4. SAXS peak widths, σ_{SAXS}, vs temperature for various cross-linking densities, X_c.

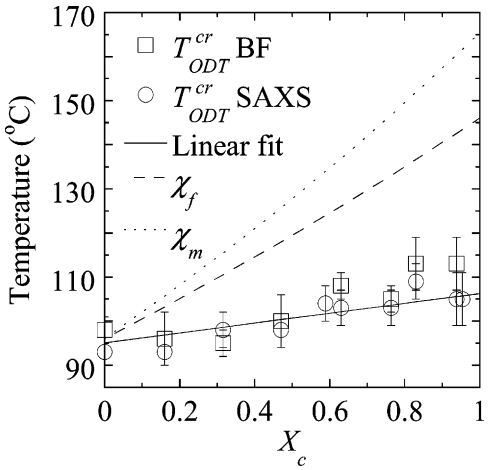

Figure 5. Temperature vs the normalized cross-linking density, X_c, phase diagram for $X_c < 1$. The squares represent experimentally measured ODTs via DPLS, the circles represent ODTs measured via SAXS and the solid line represents a linear fit to the data. The dotted lines are the theoretical results as given in eq 13 using a mean-field χ parameter, χ_m, or a fluctuation corrected χ, χ_f, from ref 23.

scattering angle) at 95 and 117 °C. Only the primary SAXS peak was observed in our samples, regardless of the value of X_c and temperature. This is not unexpected because the second order peak in our samples is severely suppressed due to the symmetry of the block copolymer ($f = 0.50$).[44] Figure 4 shows the temperature dependence of the SAXS peak width σ[45,46] obtained from samples with different values of X_c. Increasing the temperature leads to a discontinuous increase in σ in all of the samples and this is a standard signature of an order-to-disorder transition.[43] As was the case with the DPLS data, the discontinuity is less pronounced in the cross-linked samples.

Figure 5 shows the ODT temperatures measured by DPLS and SAXS for various cross-linking densities in the liquid state ($X_c < 1.00$). We have limited the range of X_c to the range where our theoretical expression (eq 13) is valid. It is clear that the ODT temperatures obtained by DPLS and SAXS for a given value of X_c are in excellent agreement. The solid line in Figure 5 is a linear fit for the dependence of T_{ODT}^{cr} on X_c.[47] The slope of the fitted line is 11.2 with a (6.5, 15.9) 95% confidence interval. The confidence interval for the slope of the linear regression line is well above zero. In Figure 5 we present the theoretical results (eq 13) using the mean field PS−PI χ parameter, $\chi_m = 0.0064 + 20/T$, and the fluctuation corrected

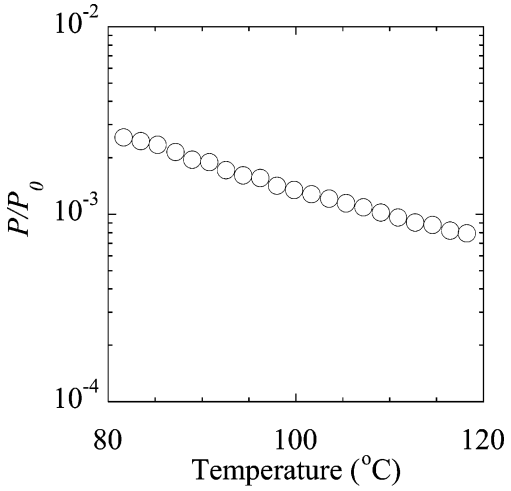

Figure 6. DPLS power vs temperature for the heating run for SI[1.27]. No ODT is observed for this sample.

χ, $\chi_f = 0.0118 + 26.5/T$.[23,48] In the literature, B values of the χ parameter vary from 20 to 74.[23,49] A B coefficient of 104 would provide quantitative agreement with experiments.

At this point we can only speculate about the reason for the lack of quantitative agreement between theory and experiment seen in Figure 5. In un-cross-linked block copolymers, the disordered state is stabilized by fluctuations and thus measured order−disorder transitions occur at temperatures lower that those predicted by mean-field theories.[50,51] It is certainly conceivable that fluctuation effects may play a much more important role in cross-linked block copolymers than un-cross-linked block copolymers. In Figure 5, we see that our data lie below the theoretical prediction obtained using the fluctuation-corrected χ parameter indicating that crude corrections based on our knowledge of un-cross-linked diblock copolymers might not be sufficient.

Equation 12 indicates that the rate of change of $(\chi N)_{ODT}^{cr}$ depends only on the volume fraction of the un-cross-linked component. Thus, the change in $T_{ODT}^{cr}$with X_c for the $f = 0.79$ sample studied in ref 12 is predicted to be less that that for the present system with f=0.50. It is apparent from the data in refs 11 and 12 that in the PS−PI block copolymer with $f = 0.79$, SI(8−24), the T_{ODT}^{cr} changes less rapidly than in SI(10−9) ($f =$ 0.50).

We have focused thus far on samples that exhibited reversible order−disorder transitions in both DPLS and SAXS experiments. In Figure 6, we show DPLS data obtained from SI[1.27] which did not show any evidence of an order−disorder transition. The SAXS data from these samples were also devoid of discontinuous changes; we do not show these for brevity. We conclude that this sample is disordered across the entire temperature window.

We now address the large difference in values of P/P_0 obtained in the ordered state in the cross-linked and un-cross-linked samples (Figure 1). This is quantified in Figure 7 where we plot the value of P/P_0 at a common temperature of 90 ± 2 °C obtained from the cooling curves vs X_c. The error bars represent the range of values obtained for at least three independent runs. The circles in Figure 7 represent data obtained from samples that exhibited a discontinuous change in P/P_0. The triangles in Figure 7 represent data from samples that did not exhibit any discontinuity in P/P_0. We see an interesting, nonmonotonic dependence of P/P_0 on X_c. In the $0.00 \leq X_c \leq 0.50$ range, P/P_0 decreases by a factor

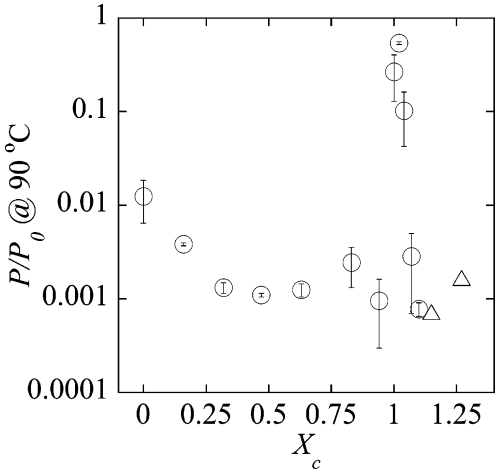

Figure 7. DPLS power at 90 °C for various cross-linking densities, X_c. There is a sudden increase in P/P_0 after crossing the gelation threshold.

of 10. This is followed by a 500-fold increase in P/P_0 in the $0.50 \leq X_c \leq 1.05$ range. Finally in the $1.05 \leq X_c \leq 1.15$ range, the value of P/P_0 again drops sharply to about 0.001. Note that 3 independent samples were made with $X_c \approx 1$ and all of the samples exhibited anomalously high values of P/P_0.

It has been established that the value of P/P_0 from unaligned block copolymers is related to the average grain size of the ordered phase, l_{av}.[39,52] In the limit of small P/P_0, l_{av} is given by

$$l_{av} = \frac{15\lambda^2}{4\pi^2(\Delta n)^2 L}\left(\frac{P}{P_0}\right) \tag{17}$$

where L is the sample thickness, Δn is the difference between the extraordinary and ordinary refractive indices, and λ is the wavelength of the incident beam. The reason for the decrease in $(P/P_0)_{90°C}$ in the $0.00 \leq X_c \leq 0.50$ range should now be clear. The creation of random cross-links in the disordered state hinders the ability of the chains to form large ordered grains. Therefore, we come to the expected conclusion that increasing the cross-linking density from 0 to 0.5 results in a 10-fold decrease in the average grain size obtained in the ordered state. However, eq 17 and the data in Figure 7 suggest that the average grain size increases by a factor of 500 when X_c is increased from 0.5 to 1.0. Equation 17 is not quantitatively valid when P/P_0 approaches unity and thus the values of l_{av} obtained using eq 17 for samples with $X_c \approx 1$ are in error. Nevertheless, the data in Figure 7 indicate that the average grain size increases by orders of magnitude as the cross-linking density approaches the gelation threshold. The increase in grain size with increasing X_c was not observed in the SI copolymer with cylindrical order studied in refs 11 and 12.

To further elucidate the nature of the ordered state of our samples we conducted TEM studies. Samples were annealed at 120 °C and then cooled at 4 °C/h until they reached 50 °C. We expect that this protocol will freeze in the grain structure of our samples just above the glass transition temperature, i.e., in the vicinity of 90 °C. In Figure 8, we show typical TEM images obtained from 4 samples: the neat SI(10−9) copolymer in Figure 8a and samples with $X_c = 0.94$, 1.02, and 1.27 in Figure 8, parts b, c, and d, respectively. The TEM images of the neat diblock were unremarkable and similar to those reported in earlier publications.[53] Long range order was evident along directions both parallel and perpendicular to the lamellar normals, as shown in Figure 8a. In the SI[0.94] sample shown in Figure 8b, we find that long range order parallel to the lamellar normals is somewhat larger than that perpendicular to them. In the SI[1.02] sample shown in Figure 8c, we see extremely anisotropic grains with good long range order parallel to the lamellar normals and very little long range order perpendicular to the lamellar normals. In the SI[1.27] sample shown in Figure 8d, we see no evidence of long range order.

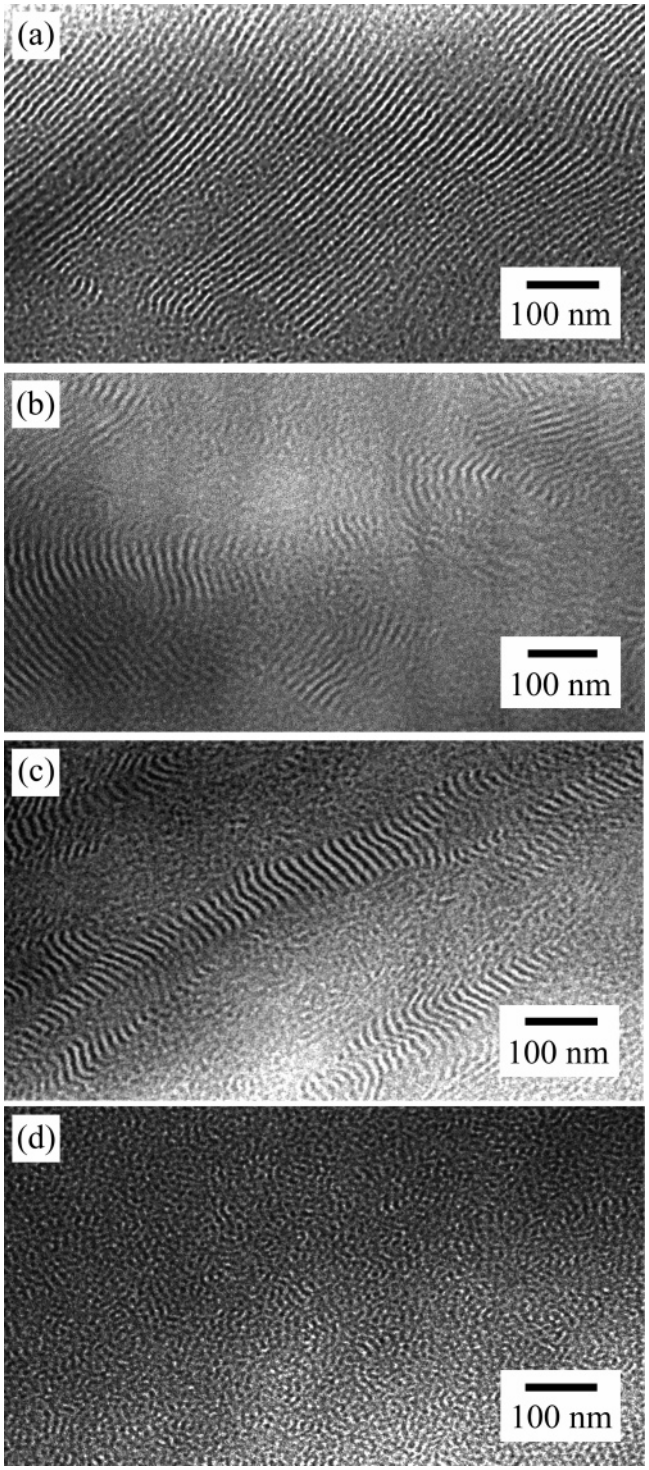

Figure 8. Typical electron micrographs of (a) SI[0.00] (no cross-linking), (b) SI[0.94], (c) SI[1.02], and (d) SI[1.27].

The combination of DPLS and TEM data indicates that near the gel point, cross-linking in the disordered state results in a very large increase in long-range order parallel to the lamellar normals. We have no explanation for this large increase in grain

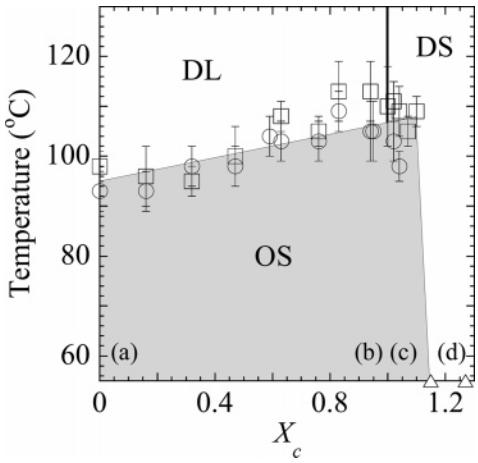

Figure 9. Temperature vs X_c phase diagram of cross-linked SI(10−9). The squares are DPLS determined ODT temperatures, the circles are SAXS determined ODT temperatures. The vertical bold line demarks the experimentally determined gelation point ($X_c = 1.00$). The gently sloped horizontal line is a linear fit to all of the ODT data, and the roughly vertical line is a linear fit to the SI[1.10] and SI[1.15] samples. The triangles are two samples which showed no presence of order in DPLS, SAXS or TEM experiments. The labels a, b, c, and d correspond to the cross-linking densities of the TEM images presented in Figure 8. The labels OS, DS, and DL denote the ordered solid, disordered solid, and disordered liquid regions of the phase diagram, respectively.

size. It is perhaps related to the critical nature of both the gelation transition and the order−disorder transition.[54] The Landau theory that we have developed is incapable of addressing the magnitude of long range order. However, the theory does predict that the ordered phase is stabilized by cross-linking, and this may serve as the starting point for uncovering the underpinning of grain structure in cross-linked block copolymers. It is conceivable that this surprising result may provide a unique insight into the nature of the gel point.

We cannot use the TEM data to quantify the changes in grain size with cross-linking density. Obtaining quantitative grain sizes of samples composed of extremely long and thin grains by TEM is virtually impossible. Even if the grains have a well-defined director that lies in one plane, it is highly unlikely that this plane will coincide with the plane of the TEM section. Figure 8c clearly shows that the director takes a curved trajectory, implying that individual TEM images are incapable of capturing entire grains. It is conceivable that electron tomography may shed light on the grain structure in our samples, but we do not have access to such instrumentation at this time.[55,56] We conducted thorough scans of the TEM images of our samples. We found many regions of highly anisotropic grains in the SI-[1.02] sample but were unable to find any such regions in the other samples.

We conclude our discussion with the phase diagram of cross-linked SI(10−9) shown in Figure 9. The distinction between order and disorder (gray vs white in Figure 9) is based on DPLS and SAXS data and confirmed by TEM. The labels a, b, c, and d in Figure 9 show the locations of the samples that were studied by TEM. The triangles represent data from samples that were disordered in our temperature window. The abbreviations OS, DS, and DL stand for ordered solid, disordered solid, and disordered liquid, respectively. The thick vertical line denotes the gelation threshold. The gently sloped horizontal line is a linear fit through the T_{ODT}^{cr} vs X_c data, while the roughly vertical line is a fit through the SI[1.10] and SI[1.15] data. Cross-linked block copolymers with X_c between 1.00 and 1.15 exhibited reversible transitions from an ordered solid to a disordered solid.

Concluding Remarks

We have used a combination of theory and experiment to study the thermodynamics and phase behavior of PS−PI block copolymers wherein the PI block is randomly cross-linked. The theory, which is restricted to cross-linking densities below the gel point ($X_c \approx 1$), predicts that cross-linking samples in the disordered state stabilizes the ordered phase, since the selective junctions corral the disordered polyisoprene chains. This surprising prediction is verified by DPLS and SAXS measurements on a symmetric poly(styrene-*block*-isoprene) copolymer. This increase in T_{ODT}^{cr} with X_c stops sharply at $X_c \approx 1$. At $X_c \geq 1.15$, the cross-linking density is high enough to prevent formation of the ordered phase. The DPLS data indicate that the long range order in cross-linked samples at the gel point ($X_c \approx 1$) along the lamellar normals is significantly larger than that obtained from both the neat un-cross-linked sample as well as samples cross-linked that are not in the vicinity of the gelation point. Theories and simulations that address the phase behavior and grain structure of cross-linked block copolymers near and above the gel point are warranted.

Acknowledgment. We acknowledge Hyeok Hahn for educational discussions and the National Center for Electron Microscopy, Ernest Orlando Lawrence Berkeley Laboratory, for use of their microscopy facilities. This work was supported by the Director, Office of Science, Office of Basic Energy Sciences, of the U.S. Department of Energy under Contract No. DE-AC03-76SF00098 and by the MRSEC Program of the National Science Foundation under Award DMR-0213618.

Appendix A. Expression for Average Cross-links Per Chain

Our derivation of an expression for the average number of cross-links per chain is similar to that in ref 29. The probability of having R number of cross-links in the system is defined as

$$P_R(\{r_{i_l}(s_l); r_{i_l'}(s_l')\}) = \frac{\mathcal{N}}{R!}\left(\frac{\mu^2}{2}\right)^R \int D(\{r_i\})\exp(-\beta H)\prod_{l=1}^{R}\upsilon_0\delta(r_{i_l}(s_l) - r_{i_l'}(s_l')) \quad \text{(A1)}$$

Therefore, the average number of cross-links is given by

$$\langle R\rangle = \left(\int D(\{r_i\})\sum_{R=1}^{\infty}\frac{R}{R!}\left(\frac{\mu^2}{2}\right)^R\sum_{i_l=1}^{m}\sum_{i_l'=1}^{m}\times \left(\prod_{l=1}^{R}\int_{Nf}^{N}\mathrm{d}s_l\int_{Nf}^{N}\mathrm{d}s_l'\upsilon_0\delta(r_{i_l}^{\alpha}(s_l) - r_{i_l'}^{\alpha}(s_l'))\right)\exp(-\beta H)\right) \Bigg/ \left(\int D(\{r_i\})\sum_{R=1}^{\infty}\frac{1}{R!}\left(\frac{\mu^2}{2}\right)^R\sum_{i_l=1}^{m}\sum_{i_l'=1}^{m}\left(\prod_{l=1}^{R}\int_{Nf}^{N}\mathrm{d}s_l\int_{Nf}^{N}\mathrm{d}s_l'\upsilon_0\delta(r_{i_l}^{\alpha}(s_l) - r_{i_l'}^{\alpha}(s_l'))\right)\exp(-\beta H)\right)$$

$$= \mu^2\frac{\partial}{\partial\mu^2}(\ln Z_1) \quad \text{(A2)}$$

In the above equation Z_1 is given by eq 6 for $n = 0$. Following the procedures described in Appendix B, one can write Z_1 as

$$Z_1 = \int D\psi(k)Dc(k)\exp(-F_0[\psi,c]) \quad \text{(A3)}$$

where $\psi(k) = f\rho_B(k) - (1 - f)\rho_A(k)$ and $c(k) = \rho_A(k) + \rho_B(k)$ denote the order parameter and the concentration variable of the system, respectively. F_0 is given by

$$F_0 = \int \frac{dk}{(2\pi)^3}[S_{cc}(k)c(k)c(-k) + S_{c\psi}(k)c(k)\psi(-k) + S_{\psi\psi}(k)\psi(k)\psi(-k) + O(c^3,\psi^3,c\psi^2,c^2\psi)] \quad \text{(A4)}$$

In the above equation

$$S_{\psi\psi}(k) = \frac{V}{m(Nv_0)^2 D}(f^2 g_2(fx) + (1-f)^2 g_2((1-f)x) + 2f(1-f)g_{12}(fx,(1-f)x)) - \frac{\mu^2}{2v_0} - \frac{\chi}{v_0} \quad \text{(A5)}$$

$$S_{c\psi} = \frac{V}{m(Nv_0)^2 D}(f g_2(fx) + (1-f) g_2((1-f)x) + (1-2f)g_{12}(fx,(1-f)x)) - \frac{(1-f)\mu^2}{2v_0} + \frac{u}{v_0} \quad \text{(A6)}$$

$$S_{cc} = \frac{V}{2m(Nv_0)^2 D}(f^2 g_2(fx) + (1-f)^2 g_2((1-f)x) - 2f(1-f)g_{12}(fx,(1-f)x)) - \frac{(1-f)^2\mu^2}{2v_0} + \frac{w}{v_0} \quad \text{(A7)}$$

D is given by eq B9 and $x = Nk^2 l_0^2/6$.

We consider the mean field solution for the disordered liquid field, $c_M(k) = \delta_{k,0}$ and $\psi_M(k) = 0$, which gives the mean field value of the average number of cross-links as

$$\langle R \rangle_M = \frac{\mu^2 mN(1-f)^2}{2} \quad \text{(A8)}$$

Our approach ignores fluctuations in the density fields, which can have contributions to the quantitative value of the average number of cross-links.

Appendix B. Derivation of Free Energy of Cross-Linked Block Copolymer Melts

In this appendix we provide details of the derivation of the free energy of cross-linked block copolymer melts. We also derive the dependence of the χ parameter (eq 12) and T_{ODT} (eq 13) on the cross-link density for the cross-linked system.

The partition function for the $(n+1)$-replica systems is described by (eq 6)

$$Z_{n+1} = \int (\prod_{\alpha=0}^{n} D\{r_i^\alpha\}) \exp\left(-\sum_{\alpha=0}^{n} \beta H^{(\alpha)} + \frac{\mu^2 N^2}{2}\sum_{i,j}^{m}\int_f^1 ds \int_f^1 ds' \prod_{\alpha=0}^{n} v_0 \delta(r_i^\alpha(s) - r_j^\alpha(s'))\right) \quad \text{(B1)}$$

where

$$H^\alpha/k_B T = \sum_{i=1}^{m} \frac{3}{2Nl_0^2}\int_0^1 ds \left(\frac{dr_i^\alpha}{ds}\right)^2 + \sum_{i,j=1}^{m}\sum_{a,b=(A,B)} \frac{\nu_{ab}^\alpha N^2}{2}\int_a ds \int_b ds'\, \delta(r_i^\alpha(s) - r_j^\alpha(s'))$$

is the standard Edwards Hamiltonian for the αth replica system. We introduce the identities $1 = \int D\rho_{(A,B)}\delta(\rho_{(A,B)} - \tilde{\rho}_{(A,B)})$ in order to write the partition function in terms of the coarse grained density variables $\rho_{(A,B)}(\hat{r})$ and $\hat{r} \equiv \{r^0, r^1, ..., r^n\}$, which represent a $3(n+1)$ dimensional vector space. The microscopic density variables, $\tilde{\rho}_{(A,B)}$, are defined as

$$\tilde{\rho}_A(\hat{r}) = N\sum_{i=1}^{m}\int_0^f ds \prod_{\alpha=0}^{n} v_0 \delta(r^\alpha - r_i^\alpha(s)) = N\sum_{i=1}^{m}\int_0^f ds\, v_0^{n+1}\delta(\hat{r} - \hat{r}_i(s)) \quad \text{(B2)}$$

$$\tilde{\rho}_B(\hat{r}) = N\sum_{i=1}^{m}\int_f^1 ds \prod_{\alpha=0}^{n} v_0 \delta(r^\alpha - r_i^\alpha(s)) = N\sum_{i=1}^{m}\int_f^1 ds\, v_0^{n+1}\delta(\hat{r} - \hat{r}_i(s)) \quad \text{(B3)}$$

After introducing the identities, the partition function is

$$Z_{n+1} = \int D\rho_A D\rho_B \delta(\rho_A - \tilde{\rho}_A)\delta(\rho_B - \tilde{\rho}_B)(\prod_{\alpha=0}^{n} D\{r_i^\alpha\}) \times \exp\left(-\sum_{\alpha=0}^{n}\sum_{i=1}^{m}\frac{3}{2Nl_0^2}\int_0^1 ds\left(\frac{dr_i^\alpha}{ds}\right)^2 - \sum_{\alpha=0}^{n}\left[\frac{\nu_{AA}^\alpha}{2v_0^2}\int dr^\alpha \rho_A^\alpha(r^\alpha)\rho_A^\alpha(r^\alpha) + \frac{\nu_{BB}^\alpha}{2v_0^2}\int dr^\alpha \rho_B^\alpha(r^\alpha)\rho_B^\alpha(r^\alpha) + \frac{\nu_{AB}^\alpha}{v_0^2}\int dr^\alpha \rho_A^\alpha(r^\alpha)\rho_B^\alpha(r^\alpha)\right] + \frac{\mu^2}{2v_0^{n+1}}\int d\hat{r}\tilde{\rho}_B(\hat{r})\tilde{\rho}_B(\hat{r})\right) \quad \text{(B4)}$$

The density variables in the αth replica system, $\rho_{(A,B)}^\alpha(r^\alpha) = v_0 N\sum_{i=1}^{m}\int_{(A,B)} ds\ \delta(r^\alpha - r_i^\alpha)$, are a subset of the variables $\tilde{\rho}_{(A,B)}(\hat{r})$. They are related as $\tilde{\rho}_{(A,B)}^\alpha(r^\alpha) = v_0^{-n}\int d\hat{x}\, \tilde{\rho}_{(A,B)}(\hat{x})\delta(x^\alpha - r^\alpha)$. We introduce auxiliary fields $\gamma_A(\hat{r})$ and $\gamma_B(\hat{r})$ to resolve the delta function constraints in the following manner: $\delta(\rho_{(A,B)}(\hat{r}) - \hat{\rho}_{(A,B)}(\hat{r})) = \int D\gamma_{(A,B)}(\hat{r}) \exp[-i\int d\hat{r}\ \gamma_{(A,B)}(\hat{r})(\rho_{(A,B)}(\hat{r}) - \hat{\rho}_{(A,B)}(\hat{r}))]$. Therefore, the partition function can be written as

$$Z_{n+1} = \int D\rho_A D\rho_B D\gamma_A D\gamma_B (\prod_{\alpha=0}^{n} D\{r_i^\alpha\}) P_A(\{\hat{r}_i\}) P_B(\{\hat{r}_i\}) \times \exp\left(-\sum_{\alpha=0}^{n}\left[\frac{\nu_{AA}^\alpha}{2v_0^2}\int dr^\alpha \rho_A^\alpha(r^\alpha)\rho_A^\alpha(r^\alpha) + \frac{\nu_{BB}^\alpha}{2v_0^2}\int dr^\alpha \rho_B^\alpha(r^\alpha)\rho_B^\alpha(r^\alpha) + \frac{\nu_{AB}^\alpha}{v_0^2}\int dr^\alpha \rho_A^\alpha(r^\alpha)\rho_B^\alpha(r^\alpha)\right] + \frac{\mu^2}{2v_0^{n+1}}\int d\hat{r}_B(\hat{r})\rho_B(\hat{r}) - i\int d\hat{r}(\gamma_A(\hat{r})\rho_A(\hat{r}) + \gamma_B(\hat{r})\rho_B(\hat{r}))\right) \quad \text{(B5)}$$

In the above expression

$$P_A(\hat{r}_i) = \sum_{j=1}^{m}\frac{3}{2Nl_0^2}\int_0^f ds\left(\frac{d\hat{r}_i}{ds}\right)^2 + \sum_{j=1}^{m} iNv_0^{n+1}\int_0^f ds\gamma_A(\hat{r}_i(s)) \text{ and}$$

$$P_B(\hat{r}_i) = \sum_{j=1}^{m}\frac{3}{2Nl_0^2}\int_f^1 ds\left(\frac{d\hat{r}_i}{ds}\right)^2 + \sum_{j=1}^{m} iNv_0^{n+1}\int_f^1 ds\gamma_B(\hat{r}_i(s))$$

Note we used $\sum_{\alpha=0}^{n}(dr_i^\alpha/ds)^2 = (d\hat{r}_i/ds)^2$in order to write the above equations.

The entropic part in the partition function originating from the integration of the chain configurations with weight factors, $P_A(\{\hat{r}_i\})$ and $P_B(\{\hat{r}_i\})$, is calculated using the Random Phase Approximation (RPA). Note the similarity in the entropic contribution between a typical diblock copolymer and the αth replica system. The entropic contribution $Q^m = (\prod_{\alpha=0}^{n} D\{r_i^\alpha\}) P_A(\{\hat{r}_i\}) P_B(\{\hat{r}_i\})$ can be expanded in a power series of the auxiliary fields $\gamma_A(\hat{r})$ and $\gamma_B(\hat{r})$ in the following manner: $Q = Q_0 + Q_1 + Q_2 + ...$, where Q_0, Q_1, and Q_2 represent the zeroth, linear, and quadratic order terms in γ_A and γ_B respectively. It turns out $Q_0 = V^{n+1}$, Q_1 is an irrelevant constant, and

$$Q_2 = -\int \frac{d\hat{k}}{(2\pi)^{n+1}} \{\gamma_A(\hat{k}) M_{AA}(\hat{k}) \gamma_A(-\hat{k}) + 2\gamma_A(\hat{k}) M_{AB}(\hat{k}) \gamma_B(-\hat{k}) + \gamma_B(\hat{k}) M_{BB}(\hat{k}) \gamma_B(-\hat{k})\} \quad \text{(B6)}$$

In the above equation

$$\gamma_{(A,B)}(\hat{k}) = \int d\hat{r} \exp(i\hat{r}\cdot\hat{k}) \gamma_{(A,B)}(\hat{r}),$$

$$M_{AA}(\hat{k}) = \frac{m(N{v_0}^{n+1})^2}{V^{n+1}} f^2 g_2(fx),$$

$$M_{BB}(\hat{k}) = \frac{m(N{v_0}^{n+1})^2}{V^{n+1}} (1-f)^2 g_2((1-f)x), \text{ and}$$

$$M_{AB}(\hat{k}) = \frac{m(N{v_0}^{n+1})^2}{V^{n+1}} f(1-f) g_{12}(fx,(1-f)x)$$

where $x = N(\hat{k}\cdot\hat{k}) l_0^2/6$, $g_2(y) = 2/y^2(y + \{\exp(-y) - 1\})$ and $g_{12}(x,y) = 1/(xy)(1 + \exp(-x - y) - \exp(-x) - \exp(-y))$. Below, we show how $M_{AA}(\hat{k})$ is calculated. Expressions for $M_{BB}(\hat{k})$ and $M_{AB}(\hat{k})$ can be obtained in a similar way.

$$(N{v_0}^{n+1})^2 (\prod_{\alpha=0}^{n} D(\{r^\alpha\})) \int_0^f ds \int_0^f ds' \gamma_A(\hat{r}(s)) \gamma_A(\hat{r}(s')) \times \exp\left(-\frac{3}{2N{l_0}^2} \int_0^f ds \left(\frac{d\hat{r}(s)}{ds}\right)^2\right)$$

$$= (N{v_0}^{n+1})^2 (\prod_{\alpha=0}^{n} D(\{r_i^\alpha\})) \int_0^f ds \int_0^f ds' \int \frac{d\hat{k}}{(2\pi)^{3(n+1)}} \gamma_A(\hat{k}) \gamma_A(-\hat{k}) \times \exp\left[-\frac{3}{2N{l_0}^2} \int_0^f ds \left(\frac{d\hat{r}_i}{ds}\right)^2 - i(\hat{k}\cdot(\hat{r}(s) - \hat{r}(s')))\right]$$

$$= (N{v_0}^{n+1})^2 \int_0^f ds \int_0^f ds' \int \frac{d\hat{k}}{(2\pi)^{3(n+1)}} \gamma_A(\hat{k}) \gamma_A(-\hat{k}) \times \langle \exp[-i(\hat{k}\cdot(\hat{r}(s) - \hat{r}(s')))]\rangle_0$$

$$= (N{v_0}^{n+1})^2 \int_0^f ds \int_0^f ds' \int \frac{d\hat{k}}{(2\pi)^{3(n+1)}} \gamma_A(\hat{k}) \gamma_A(-\hat{k}) \times \exp[-(k^2 \langle (\hat{r}(s) - \hat{r}(s'))^2\rangle_0)]$$

$$= (N{v_0}^{n+1})^2 \int_0^f ds \int_0^f ds' \int \frac{d\hat{k}}{(2\pi)^{3(n+1)}} \gamma_A(\hat{k}) \gamma_A(-\hat{k}) \times \exp\left[-\frac{k^2 N{l_0}^2}{6} |s - s'|\right]$$

$$= (N{v_0}^{n+1})^2 \int \frac{d\hat{k}}{(2\pi)^{3(n+1)}} \gamma_A(\hat{k}) \gamma_A(-\hat{k}) g_2\left(\frac{f^2 k^2 N{l_0}^2}{6}\right)$$

In the above equation, $\langle ... \rangle_0$, refers to the configuration average with a weight of $\exp(-3/2N{l_0}^2 \int_0^1 ds\, (dr(s)/ds)^2)$. Therefore, the partition function can be written as

$$Z_{n+1} = \int D\rho_A D\rho_B D\gamma_A D\gamma_B \times \exp\left(-\int \frac{d\hat{k}}{(2\pi)^{3(n+1)}} \gamma^T \mathbf{M} \gamma + O({\gamma_A}^3, {\gamma_B}^3, {\gamma_A}^2\gamma_B, \gamma_A{\gamma_B}^2) - \sum_{\alpha=0}^{n} \left[\frac{\nu_{AA}^\alpha}{2{\nu_0}^2} \int \frac{dk^\alpha}{(2\pi)^3} \rho_A^\alpha(k^\alpha) \rho_A^\alpha(-k^\alpha) + \frac{\nu_{BB}^\alpha}{2{\nu_0}^2} \int \frac{dk^\alpha}{(2\pi)^3} \rho_B^\alpha(k^\alpha) \rho_B^\alpha(-k^\alpha) + \frac{\nu_{AB}^\alpha}{{\nu_0}^2} \int \frac{dk^\alpha}{(2\pi)^3} \rho_A^\alpha(k^\alpha) \rho_B^\alpha(-k^\alpha)\right] + \frac{\mu^2}{2{\nu_0}^{n+1}} \int \frac{d\hat{k}}{(2\pi)^{3(n+1)}} \rho_B(\hat{k}) \rho_B(-\hat{k}) - i \int \frac{d\hat{k}}{(2\pi)^{3(n+1)}} (\gamma_A(\hat{k}) \rho_A(-\hat{k}) + \gamma_B(k) \rho_A(-\hat{k})) \quad \text{(B7)}$$

Here $\gamma \equiv (\gamma_A, \gamma_B)$ and

$$\mathbf{M} \equiv \begin{pmatrix} M_{AA} & M_{AB} \\ M_{AB} & M_{BB} \end{pmatrix}$$

We perform a saddle point approximation to calculate the integrals in the auxiliary fields and obtain

$$Z_{n+1} = \int D\rho_A D\rho_B \times \exp\left(-\int \frac{d\hat{k}}{(2\pi)^{3(n+1)}} \rho^T \mathbf{M}^{-1} \rho + O({\rho_A}^3, {\rho_B}^3, {\rho_A}^2\rho_B, \rho_A{\rho_B}^2) - \sum_{\alpha=0}^{n} \left[\frac{\nu_{AA}^\alpha}{2{\nu_0}^2} \int \frac{dk^\alpha}{(2\pi)^3} \rho_A^\alpha(k^\alpha) \rho_A^\alpha(-k^\alpha) + \frac{\nu_{BB}^\alpha}{2{\nu_0}^2} \int \frac{dk^\alpha}{(2\pi)^3} \rho_B^\alpha(k^\alpha) \rho_B^\alpha(-k^\alpha) + \frac{\nu_{AB}^\alpha}{{\nu_0}^2} \int \frac{dk^\alpha}{(2\pi)^3} \rho_A^\alpha(k^\alpha) \rho_B^\alpha(-k^\alpha)\right] + \frac{\mu^2}{2{\nu_0}^{n+1}} \int \frac{d\hat{k}}{(2\pi)^{3(n+1)}} \rho_B(\hat{k}) \rho_B(-\hat{k}) \quad \text{(B8)}$$

In the above equation, $\rho \equiv (\rho_A, \rho_B)$ and

$$\mathbf{M}^{-1} \equiv \begin{pmatrix} W_{AA} & W_{AB} \\ W_{AB} & W_{BB} \end{pmatrix}$$

where

$$W_{AA} = \frac{V^{n+1}}{m(N{v_0}^{n+1})^2 D} f^2 g_2(fx),$$

$$W_{BB} = \frac{V^{n+1}}{m(N{v_0}^{n+1})^2 D} (1-f)^2 g_2((1-f)x),$$

$$W_{AB} = \frac{V^{n+1}}{m(N{v_0}^{n+1})^2 D} f(1-f) g_{12}(fx,(1-f)x),$$

and

$$D = f^2(1-f)^2 [g_2(fx) g_2((1-f)x) - (g_{12}(fx,(1-f)x))^2] \quad \text{(B9)}$$

We define the order parameters $\psi(\hat{k}) = (1-f)\rho_A(\hat{k}) - f\rho_B(\hat{k})$ and $c(\hat{k}) = \rho_A(\hat{k}) + \rho_B(\hat{k})$. In terms of the order parameters,

$$Z_{n+1} = \int D\psi(\hat{k}) Dc(\hat{k}) \exp(-\tilde{F}[\psi,c])$$

$$\tilde{F} = \int \frac{d\hat{k}}{(2\pi)^{3(n+1)}} (\Gamma_{\psi\psi} \psi(\hat{k}) \psi(-\hat{k}) + \Gamma_{\psi c} \psi(\hat{k}) c(-\hat{k}) + \Gamma_{cc} c(\hat{k}) c(-\hat{k})) + O(\psi^3, c^3, c\psi^2, \psi c^2) \quad \text{(B10)}$$

where

$$\Gamma_{\psi\psi} = \frac{V^{n+1}}{m(N{v_0}^{n+1})^2 D}(f^2 g_2(fx) + (1-f)^2 g_2((1-f)x) + 2f(1-f)g_{12}(fx,(1-f)x)) - \frac{\mu^2}{2{v_0}^{n+1}} - \frac{1}{{v_0}^{2n+1}}\sum_{\alpha=0}^{n}\chi^{(\alpha)}\prod_{\beta=0,\beta\neq\alpha}^{n}\delta(k^\beta) \quad \text{(B11)}$$

$$\Gamma_{c\psi} = \frac{V^{n+1}}{m(N{v_0}^{n+1})^2 D}(f g_2(fx) + (1-f)g_2((1-f)x) + (1-2f)g_{12}(fx,(1-f)x)) - \frac{(1-f)\mu^2}{2{v_0}^{n+1}} + \frac{1}{{v_0}^{2n+1}}\sum_{\alpha=0}^{n}u^{(\alpha)}\prod_{\beta=0,\beta\neq\alpha}^{n}\delta(k^\beta) \quad \text{(B12)}$$

$$\Gamma_{cc} = \frac{V^{n+1}}{2m(N{v_0}^{n+1})^2 D}(f^2 g_2(fx) + (1-f)^2 g_2((1-f)x) - 2f(1-f)g_{12}(fx,(1-f)x)) - \frac{(1-f)^2\mu^2}{2{v_0}^{n+1}} + \frac{1}{{v_0}^{2n+1}}\sum_{\alpha=0}^{n}w^{(\alpha)}\prod_{\beta=0,\beta\neq\alpha}^{n}\delta(k^\beta) \quad \text{(B13)}$$

Since the system was cross-linked in the disordered state, $\psi^{(0)}(k^{(0)}) = 0$ and $c^{(0)}(k^{(0)}) = \delta_{k^{(0)},0}$. Therefore, if we replace $\psi(\hat{k})$ and $c(\hat{k})$ by their values which minimize the free energy $\tilde{F}[\psi,c]$ we get $\underset{n\to 0}{Lt}\frac{F_n}{n} = -\beta^{-1}\underset{n\to 0}{Lt}\frac{Z_{\mathbf{n}+1} - Z_1}{nZ_1}$ where F_n is given by eq 8.

To investigate the stability of different phases, we need to expand the order parameters in single and many replica sectors as described in eq 7 and calculate the free energy $F = \underset{n\to 0}{Lt}\frac{F_n}{n}$. The conditions $\partial F/\partial\psi|_{c=c_M;\psi=\psi_M} = \partial F/\partial c|_{c=c_M;\psi=\psi_M} = 0$ and $\partial^2 F/\partial\psi^2|_{c=c_M;\psi=\psi_M} > 0$, $\partial^2 F/\partial c^2|_{c=c_M;\psi=\psi_M} > 0$, $\partial^2 F/\partial c\partial\psi|_{c=c_M;\psi=\psi_M} > 0$ are used to calculate the stable minimum energy phases (c_M,ψ_M) and the condition $F(\psi = \psi_M, c = c_M,\chi_{ODT}) = F_{dis}$, where F_{dis} is the free energy of the system in the disordered liquid state, can be used to calculate T_{ODT} or χ_{ODT}. It is clear from the expansion of Γ_{cc} as $\hat{k}\cdot\hat{k}\to 0$, $\Gamma_{cc}\to V^{n+1}/2m(N{v_0}^{n+1})^2 - (1-f)^2\mu^2/2{v_0}^{n+1} + O(\hat{k}.\hat{k})$, that a liquid state $(\bar{c}(\hat{k}) = 0)$ becomes unstable for $(1-f)^2\mu^2/2v_0 > V/2m(Nv_0)^2$, i.e., $(1-f)^2\mu^2 N > 1$ or $n_c > 1/2$.

From the expansion of $\Gamma_{\psi\psi}$

$$\Gamma_{\psi\psi} = \frac{V^{n+1}}{m(N{v_0}^{n+1})^2 D}(f^2 g_2(fx) + (1-f)^2 g_2((1-f)x) + 2f(1-f)g_{12}(fx,(1-f)x)) - \frac{\mu^2}{2{v_0}^{n+1}} - \frac{1}{{v_0}^{2n+1}}\sum_{\alpha=0}^{n}\chi^{(\alpha)}\prod_{\beta=0,\beta\neq\alpha}^{n}\delta(k^\beta) \quad \text{(B14)}$$

it is evident that the disordered phase in $\psi^\alpha(k^\alpha)$ becomes unstable for temperatures that will make $V\chi_{min}/(2m(Nv_0)^2) - \mu^2/(2v_0) - \chi/v_0 < 0$, where χ_{min} is the minimum value of the k^α dependent part of $\Gamma^{(\alpha)}(k^\alpha)$ at a wave vector ${k_m}^\alpha \propto 1/(Nl_0^2)^{1/2}$, which determines the phase separation length scale in the diblock copolymer system. Therefore, if we consider the free energy up to the quadratic power in the order parameters, $(\chi N)_{ODT}^{cr} = \chi_{min}/2 - \mu^2 N/2$. In absence of any cross-linking, $(\chi N)_{ODT} = \chi_{min}/2$. Thus, we get eq 12 as a relation between the χN parameter when the system is cross-linked and un-cross-linked.

Following the same approach and taking $\chi = A + B/T$, we find that the disordered phase becomes unstable for temperatures $V\chi_{min}/(2m(Nv_0)^2) - \mu^2/(2v_0) - (A + B/T)/v_0 < 0$. Thus, $N(A + B/T_{ODT}^{cr}) = \chi_{min}/2 - \mu^2 N/2$. However, $N(A + B/T_{ODT}) = \chi_{min}/2$; therefore, we get eq 13 as a relationship between T_{ODT}^{cr} and T_{ODT}. We assume that A and B do not change when cross-links are introduced.

References and Notes

(1) Flory, P. J. *Principles of Polymer Chemistry*; Cornell University Press: Ithaca, NY, 1953.
(2) Graessley, W. W. *Polymeric Liquids and Networks: Structure and Properties*; Garland Science: New York, 2004.
(3) Won, Y. Y.; Davis, H. T.; Bates, F. S. *Science* **1999**, *283*, 960−963.
(4) Thurmond, K. B.; Kowalewski, T.; Wooley, K. L. *J. Am. Chem. Soc.* **1996**, *118*, 7239−7240.
(5) Butun, V.; Billingham, N. C.; Armes, S. P. *J. Am. Chem. Soc.* **1998**, *120*, 12135−12136.
(6) Emoto, K.; Iijima, M.; Nagasaki, Y.; Kataoka, K. *J. Am. Chem. Soc.* **2000**, *122*, 2653−2654.
(7) Ding, J. F.; Liu, G. J. *Macromolecules* **1998**, *31*, 6554−6558.
(8) Durkee, D. A.; Eitouni, H. B.; Gomez, E. D.; Ellsworth, M. W.; Bell, A. T.; Balsara, N. P. *Advanced* Materials **2005**, *17*, 2003−2006.
(9) Hillmyer, M. A.; Lipic, P. M.; Hajduk, D. A.; Almdal, K.; Bates, F. S. *J. Am. Chem. Soc.* **1997**, *119*, 2749−2750.
(10) Sakurai, S.; Iwane, K.; Nomura, S. *Macromolecules* **1993**, *26*, 5479−5486.
(11) Hahn, H.; Eitouni, H. B.; Balsara, N. P.; Pople, J. A. *Phys. Rev. Lett.* **2003**, *90*, 155505.
(12) Hahn, H.; Chakraborty, A. K.; Das, J.; Pople, J. A.; Balsara, N. P. *Macromolecules* **2005**, *38*, 1277−1285.
(13) Deam, R. T.; Edwards, S. F. *Philos. Trans. R. Soc A* **1976**, *280*, 317−353.
(14) Edwards, S. F.; Vilgis, T. A. *Rep. Prog. Phys.* **1988**, *51*, 243−297.
(15) Binder, K. *Monte Carlo and Molecular Dynamics Simulations in Polymer Science*; Oxford University Press: Oxford, U.K., 1995.
(16) Leibler, L. *Macromolecules* **1980**, *13*, 1602−1617.
(17) Hamley, I. W. *The Physics of Block Copolymers*; Oxford University Press: Oxford, U.K., 1998.
(18) Stepanow, S.; Schulz, M.; Binder, K. *J. Phys. Ii* **1994**, *4*, 819−824.
(19) Uchida, N. *J. Phys. Condens. Matter* **2004**, *16*, L21-L27.
(20) Lay, S.; Sommer, J. U.; Blumen, A. *J. Chem. Phys.* **1999**, *110*, 12173−12182.
(21) Doi, M.; Edwards, S. F. *The Theory of Polymer Dynamics*; Oxford University Press: Oxford, U.K., 1986.
(22) Doi, M. *Introduction to Polymer Physics*; Oxford University Press: New York, 1996.
(23) Lin, C. C.; Jonnalagadda, S. V.; Kesani, P. K.; Dai, H. J.; Balsara, N. P. *Macromolecules* **1994**, *27*, 7769−7780.
(24) The Gibbs prefactor is chosen as $1/(m!)$ and is strictly valid in the un-cross-linked sample. However, in the presence of cross-links, as rightly noted in ref 28, the system will contain various cross-linked clusters which will change the Gibbs prefactor, $1/(m!)$. The form of the correct Gibbs prefactor is not known and is difficult to compute. Therefore we retain the prefactor as the un-cross-linked system and our results do not depend on the choice of Gibbs prefactor.
(25) Cardy, J. L. *Scaling and Renormalization in Statistical Physics*; Cambridge University Press: New York, 1996.
(26) Binder, K.; Young, A. P. *Rev Mod Phys* **1986**, *58*, 801−976.
(27) Edwards, S. F.; Anderson, P. W. *J. Phys. F, Met. Phys.* **1975**, *5*, 965−974.
(28) Goldbart, P. M.; Castillo, H. E.; Zippelius, A. *Adv. Phys.* **1996**, *45*, 393−468.
(29) Roos, C.; Zippelius, A.; Goldbart, P. M. *J. Phys. A., Math. Gen.* **1997**, *30*, 1967−1977.
(30) Ohta, T.; Kawasaki, K. *Macromolecules* **1986**, *19*, 2621−2632.
(31) Gutin, A. M.; Shakhnovich, E. I. *J. Chem. Phys.* **1994**, *100*, 5290−5293.
(32) Panyukov, S.; Rabin, Y. *Phys. Rep.* **1996**, *269*, 1−131.

(33) Gonzalez, L.; Rodriguez, A.; Marcos, A.; Chamorro, C. *Rubber Chem. Technol.* **1996**, *69*, 203-214.
(34) Queslel, J. P.; Mark, J. E. *J. Chem. Phys.* **1985**, *82*, 3449−3452.
(35) Queslel, J. P.; Fontaine, F.; Monnerie, L. *Polymer* **1988**, *29*, 1086−1090.
(36) Mark, J. E.; Erman, B. *Rubberlike Elasticity: A Molecular Primer*; John Wiley & Sons: New York, 1988.
(37) Erman, B.; Mark, J. E. *Structures and Properties of Rubberlike Networks*; Oxford University Press: New York, 1997.
(38) The network density ($\rho = 0.978$, $\rho_{PS} = 1.036$, and $\rho_{PI} = 0.912$ g/cm^3; see ref 23) was assumed to be the weight average of the two homopolymer densities at 25 °C, and the χ_{SP} parameter ($\chi_{SP} = 0.385$, $\chi_{SP,PS} = 0.41$, and $\chi_{SP,PI} = 0.36$; see ref 12) describing the interactions between the block copolymer networks and toluene was assumed to be the volume average of the two homopolymer χ's. The molar volume of toluene is 106.5 mL/mol.
(39) Garetz, B. A.; Newstein, M. C.; Dai, H. J.; Jonnalagadda, S. V.; Balsara, N. P. *Macromolecules* **1993**, *26*, 3151−3155.
(40) Eitouni, H. B.; Balsara, N. P.; Hahn, H.; Pople, J. A.; Hempenius, M. A. *Macromolecules* **2002**, *35*, 7765−7772.
(41) The accuracy of the calibration was subsequently checked with a different disordered block copolymer, poly(isoprene-*block*-ferrocenyldimethylsilane) copolymer with weight-averaged molecular weights of 8 and 10 kg/mol, respectively.
(42) Russell, T. P.; Lin, J. S.; Spooner, S.; Wignall, G. D. *J. Appl. Crystallogr.* **1988**, *21*, 629−638.
(43) Perahia, D.; Vacca, G.; Patel, S. S.; Dai, H. J.; Balsara, N. P. *Macromolecules* **1994**, *27*, 7645−7649.
(44) Roe, R.-J. *Methods of X-ray and Neutron Scattering in Polymer Science*; Oxford University Press: New York, 2000.
(45) Eitouni, H. B.; Balsara, N. P. *J. Am. Chem. Soc.* **2004**, *126*, 7446−7447.
(46) The primary peak (ca. $q = 0.43$ nm^{-1}) is assumed to be of the form $I(q) = C \exp[-(q - q_{peak})^2/\sigma^2] + I_{bgd}$ and the peak width at half-maximum is determined by fitting this assumed form to the scattering data. I_{bgd} is assumed to be a q-independent constant.
(47) As the cross-linking density was increased, T_{ODT} becomes less sharply defined, as can be seen in Figure 2. Thus, the error in the T_{ODT} measurement increased with cross-linking density.
(48) N (233) and χ are based on a reference volume of 150.3 Å^3. $\phi = 0.5$, and $T_{ODT} = 369$ K, the average of the DPLS and SAXS determined ODT temperatures.
(49) Abuzaina, F. M.; Patel, A. J.; Mochrie, S.; Narayanan, S.; Sandy, A.; Garetz, B. A.; Balsara, N. P. *Macromolecules* **2005**, *38*, 7090−7097.
(50) Fredrickson, G. H.; Helfand, E. *J. Chem. Phys.* **1987**, *87*, 697−705.
(51) Maurer, W. W.; Bates, F. S.; Lodge, T. P.; Almdal, K.; Mortensen, K.; Fredrickson, G. H. *J. Chem. Phys.* **1998**, *108*, 2989−3000.
(52) Balsara, N. P.; Garetz, B. A.; Dai, H. J. *Macromolecules* **1992**, *25*, 6072−6074.
(53) Garetz, B. A.; Balsara, N. P.; Dai, H. J.; Wang, Z.; Newstein, M. C.; Majumdar, B. *Macromolecules* **1996**, *29*, 4675−4679.
(54) de Gennes, P. G. *Scaling Concepts in Polymer Physics*; Cornell University Press: Ithaca, NY, 1979.
(55) Mcewen, B. F.; Downing, K. H.; Glaeser, R. M. *Ultramicroscopy* **1995**, *60*, 357−373.
(56) Spontak, R. J.; Fung, J. C.; Braunfeld, M. B.; Sedat, J. W.; Agard, D. A.; Ashraf, A.; Smith, S. D. *Macromolecules* **1996**, *29*, 2850−2856.

MA052323R